International Journal of GEOMATE, Nov, 2022, Vol.23, Issue 99, pp.119-125
ISSN: 2186-2982 (P), 2186-2990 (O), Japan, DOI: https://doi.org/10.21660/2022.99.s8508
Geotechnique, Construction Materials and Environment

A NEW TYPE OF ELECTROMAGNETIC-VIBRATION-TYPE SMALL PUMP WITH HIGH EFFICIENCY

* Hiroyuki Yaguchi[1], Takuya Watanabe[1] and Toshiki Mishina[1]

[1]Faculty of Engineering, Tohoku Gakuin University, Japan

*Corresponding Author, Received: 01 Aug. 2022, Revised: 07 Sept. 2022, Accepted: 20 Oct. 2022

ABSTRACT: Small pumps with excellent performance are in demand in various industrial fields. In the present study, a new type of small underwater insertion pump that combines electromagnetic force and mechanical resonance was developed. A prototype electromagnetic-vibration pump with a one-valve structure in which the vibration component and water are separated by a thin film was constructed. The shape of this pump was optimally designed for the casing and valves. Rod and piston-type casings have been proposed to effectively use the displacement of the vibration component. By the inertial effect of water due to the operating principle, thin film separation, and shape optimization, the maximum efficiency of this pump was 19.1%, which exceeds that of previously proposed small pumps. In addition, as a normal use of the prototype pump, the pump with an acrylic pipe attached to the inlet port was improved, and its flow rate characteristics were examined. These two pumps can be directly driven by the power of a power outlet by tuning the resonance frequency of the vibration component. The proposed pump can be used in two ways depending on the application.

Keywords: Pump, Vibration, One-valve pump, Optimized shape, Pumping head, Efficiency, Mass flow.

1. INTRODUCTION

Small pumps with excellent performance are in high demand in various industrial fields, such as the fields of machinery, civil engineering, agriculture, chemical analysis, and medical care. For this reason, various types of small pumps have been developed. In particular, the axial flow pump [1], centrifugal pump [2 - 4], and rotary pumps [5 - 8] have been actively studied. An electromagnetic motor is used as a drive source for these pumps because the efficiency of the pump depends on the efficiency of the electromagnetic motor. Accordingly, due to the low efficiency of the small motors installed, the efficiency of the small pumps is quite low.

A piezoelectric pump [9 - 11] is a typical pump that does not use an electromagnetic motor. Although this pump is characterized by high efficiency, it has a problem with respect to durability and is expensive. Even so, the efficiency of the small piezoelectric pump is less than 5%.

Therefore, considering environmental problems of note in recent years, pumps and motors are incorporated in many devices, and improving the efficiency of these basic devices is an important engineering problem.

For this reason, the authors prototyped a vibration-type pump [12], in which a drive unit having a vibration component was inserted into water, and showed the flow rate characteristics of the prototype pump. However, the efficiency of this pump is low, and the operation principle has not been clarified.

In the present study, a new type of small underwater insertion pump that combines electromagnetic force and mechanical resonance was developed. This small vibration-type pump converts the generated resonance energy into kinetic energy and effectively discharges water. A prototype pump with a one-valve structure in which the vibration component and water are separated by a thin film was prototyped. The shape of this pump was optimally designed with respect to the casing and valves. Rod and piston-type casings have been proposed to effectively use the displacement of the vibration component. By the inertial effect of water due to the operating principle, thin film separation, and shape optimization, the maximum efficiency of this pump was 19.1%, which exceeds that of previously proposed small pumps. In addition, as a normal use of the prototype pump, the pump with an acrylic pipe attached to the inlet port was improved, and its flow rate characteristics were examined. It was clarified that this small vibration-type pump has a very simple structure and can discharge water with a pumping head exceeding 1,000 mm. Two types of pump with high performances capable of use in two ways are described in the present paper.

2. RESEARCH SIGNIFICANCE

Considering the global environment, improving the efficiency of small motors and

pumps installed in various devices is an important issue. Currently, the efficiencies of commercially available small pumps are less than about 5%. Therefore, there is a need to significantly improve the efficiency of small pumps. In this paper, we developed a novel vibration-type small pump and established a new operating principle. The efficiency of this vibration pump is about 20%, and its applicability to various industrial fields was verified. A significant reduction in power can be achieved by proposing two types of small pumps.

3. OUTLINE OF THE VIBRATION-TYPE PUMP

Fig. 1 shows a small electromagnetic-vibration pump for an underwater insertion-type pump. This vibration-type pump consists of an acrylic casing, a thin silicone rubber film, a vibration component, an acrylic bar, and a discharge valve. In this pump, a thin silicone rubber film with a thickness of h (mm) was installed on top of the vibration component to prevent contact between water and the vibration component. The part above the silicone rubber film is defined as the head portion, and the portion below the silicone rubber film is defined as the vibration portion. As a result, water flows into the head portion, and only air is injected into the vibration portion. Since the vibration component vibrates in the atmosphere, no viscous resistance of water is generated. The valve is a one-valve system with only discharge and has a very simple structure.

The acrylic rod and piston-type casings have been developed to effectively use the displacement of the vibration component. An inlet port and an outlet port having a diameter of 6 mm are attached to the head part, as shown in Fig. 1.

The vibration component consists of a ring-shaped permanent magnet and a compression coil spring. The permanent magnet is a neodymium ring magnet with an outer diameter of 12 mm, an inner diameter of 9 mm, and a height of 5 mm. As the spring, a compression coil spring with a free length of 25 mm, an outer diameter of 12 mm, and a spring constant of k = 2,691 N/m was used.

As shown in Fig. 2, an iron core with a bobbin shape was used as an electromagnet for exciting the vibration component. A copper wire with a diameter of 0.2 mm was wound 1,200 times to make an electromagnet. By combining a ring-type permanent magnet and the bobbin-type permanent magnet, the electromagnetic force can be efficiently converted into excitation force [13 - 15]. As shown in Fig. 2, for the iron disk, the diameter is R = 8 mm, and the thickness is b = 1 mm. In addition, the shaft diameter is r = 3 mm, and the length is B = 26 mm. The acrylic bar was mounted on the vibration component to increase the effect of pushing up the water.

Fig. 3 shows the structure and dimensions of the valve. A triangular acrylic support was

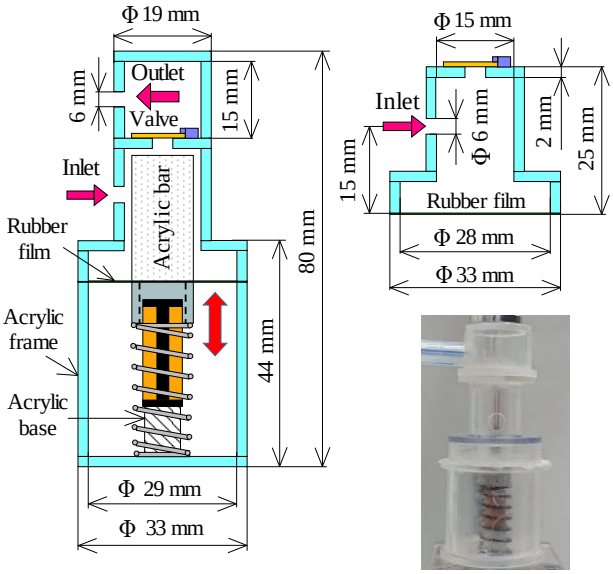

(a) Outline (b) Head portion and photograph

Fig. 1 Structure of the vibration-type pump

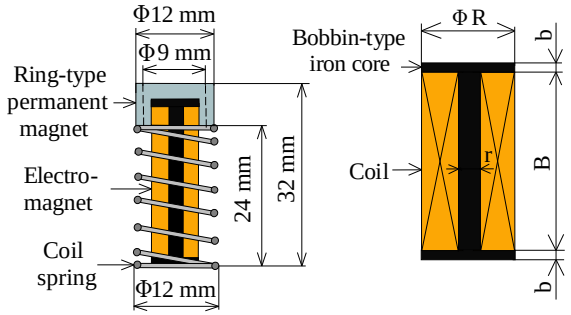

Fig. 2 Vibration component and electromagnet

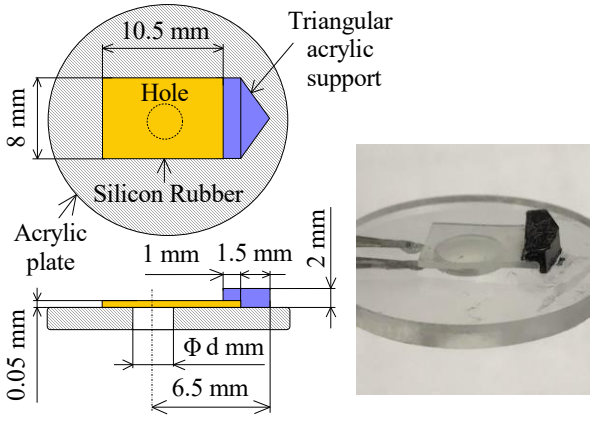

Fig. 3 Structure of the one-valve pump and photograph

attached to an acrylic disc with a thickness of 2 mm, an outer diameter of 19 mm, and an inner diameter of d (mm). The dimensions of the thin silicone rubber material for the valve are 8 mm wide, 10.5 mm long, and 0.05 mm thick. By attaching a thin silicone material to the triangular acrylic support, stable bending rigidity in the valve was obtained.

This pump is inserted into water, and AC power is input to the bobbin-type electromagnet to resonate the vibration component. An acrylic bar with a diameter of 12 mm and a length of L (mm) attached to the top of the vibration component via the silicone rubber film vibrates in the vertical direction. As shown in Fig. 1, when the acrylic bar is displaced upward, the pressure near the valve increases. The thin silicone material in the valve is pushed up, and water is drained. On the other hand, when the acrylic bar is displaced downward, the pressure near the valve decreases. For this reason, the valve closes and prevents backflow of water. Thus, since the pressure at the head portion is reduced, water can be sucked up from the inlet port. Based on the results of a previous study [12], a clearance of 1.5 mm was provided between the rod and the casing so that water could flow between them. Water is discharged intermittently by repeatedly increasing and decreasing the pressure over one cycle of vibration.

As shown in Fig. 1, the dimensions of the head portion are when the length of the acrylic bar is 25 mm. The prototype pump has a height of 80 mm, an outer diameter of 33 mm, and a total mass of 41 g.

4. OPTIMUM DESIGN FOR THE SHAPE OF THE VIBRATION-TYPE PUMP

As shown in Fig. 1, the shape of the vibration-type pump for an underwater insertion-type was optimized for the following three items:

(1) Length of the acrylic rod: L (mm)
(2) Thickness of the silicone rubber film for water separation: h (mm)
(3) Diameter of the outlet port in the valve: d (mm)

The prototype pump was inserted into an acrylic tank having a width of 350 mm, a length of 250 mm, and a height of 200 mm.

As shown in Fig. 4, the pumping head was 200 mm, and the flow rate was measured. An acrylic pipe with an inner diameter of 6 mm was used as the pipe from the outlet port. The vibration component was driven at the resonance frequency by a signal generator and amplifier. The resonance frequency is 70 Hz. The input voltage, current, and power to the electromagnet were measured using a power analyzer. The mass of discharged water was measured for 30 seconds using an electronic balance. The water temperature was measured as 20 degrees.

The pumping head (H = 200 mm), the diameter (d = 4 mm) of the outlet port in the valve, the thickness (h = 0.01 mm) of the silicon thin film, and the effect of the length, L (mm), of the acrylic rod were examined. Fig. 5 shows the relationship between the input power to the electromagnet and the flow rate per second by changing the length, L (mm), of the acrylic rod to 15 mm, 25 mm, and 30 mm. The highest efficiency was shown when the rod length was 25 mm. This indicates the existence of an optimum rod length. As the rod length increases, the effect of pushing out water increases. However, as the rod length increases, the contact area between the water and the rod increases and the viscous resistance to the vibration component increases. Therefore, it is considered that the optimum length of the rod exists.

The effects of the thickness, h (mm), of the silicone rubber film for water separation were examined with the pumping head (H = 200 mm), length (L = 25 mm) of the acrylic rod, and the outlet port diameter of the valve (d = 4 mm). Fig. 6 shows the relationship between the input power to

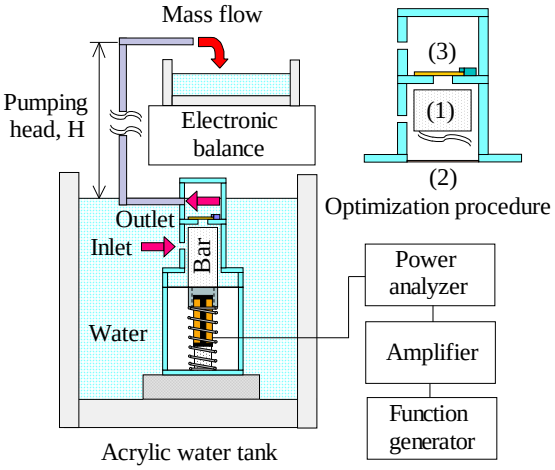

Fig. 4 Experimental apparatus and optimization procedure

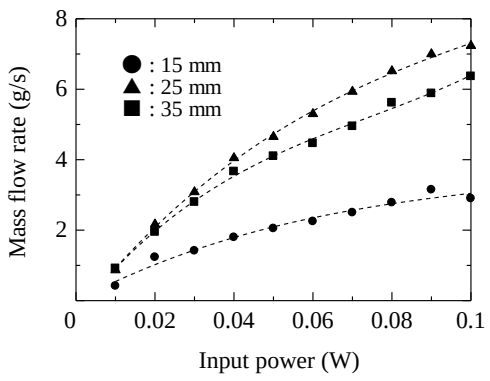

Fig. 5 Relationship between input power and mass flow rate (length of the acrylic rod)

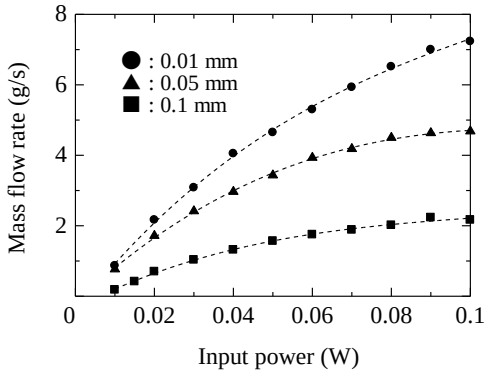

Fig. 6 Relationship between input power and mass flow rate (thickness of the silicone rubber film)

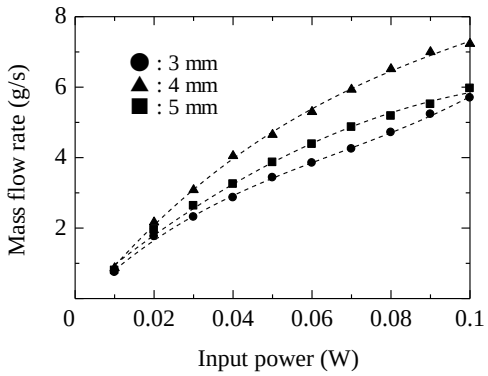

Fig. 7 Relationship between input power and mass flow rate (diameter of outlet port)

the electromagnet and the flow rate per second by varying the thickness, h (mm), of the thin silicone rubber film to 0.01 mm, 0.05 mm, and 0.1 mm. From the figure, the flow rate increases as the input power increases. When the silicone rubber film thickness is thin, this pump shows good flow rate characteristics. As the silicone rubber film thickness increases, the viscous resistance of the membrane material to the vibration component increases. Therefore, when the silicone rubber with a thickness of h = 0.01 mm is used, the flow rate characteristics are the best.

The pumping head (H = 200 mm), the length (L = 25 mm) of the acrylic rod, the silicon thin film thickness (h = 0.01 mm), and the effect of hole diameter, d (mm), at the outlet port in the valve were examined. Fig. 7 shows the relationship between the input power to the electromagnet and the flow rate per second by varying the hole diameter, d (mm), of the outlet port in the valve as 3 mm, 4 mm, and 5 mm. From the figure, the highest efficiency occurs when the hole diameter is 4 mm. However, the diameter of the hole in the valve portion is considered to be affected by the pumping head.

By examining three items, the value of (1) the length (L = 25 mm) for the acrylic rod, (2) the thickness (h = 0.01 mm) for the silicone rubber film for water separation, and (3) the diameter (d = 4 mm) for the outlet port in the valve are selected to maximize the flow characteristics of this pump.

5. INERTIA EFFECT DUE TO VIBRATION DISPLACEMENT OF THE ROD

This pump creates a pressure difference by the combination of the acrylic rod and the casing. Water cannot be sucked in and drained if the acrylic rod is not mounted on the vibration component at this pump. In addition, if the clearance between the acrylic rod and the casing is 0 mm, then water cannot be sucked from the inlet port. As mentioned above, the clearance between the rod and the casing was set to 1.5 mm, and the water discharge characteristics due to the vibration displacement of the rod were examined.

It is difficult to directly measure the displacement of a vibration component inserted in water with various sensors. The displacement was measured using the experimental apparatus shown in Fig. 8. In the experiment, the sine wave generated by the signal generator was amplified by an amplifier, and the exciter was vibrated harmonically. The vibration part of the exciter, two

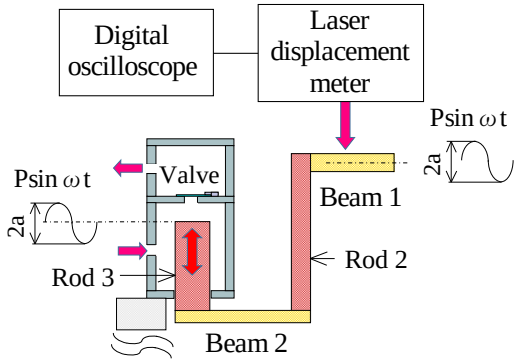

Fig. 8 Experimental setup for the operating principle

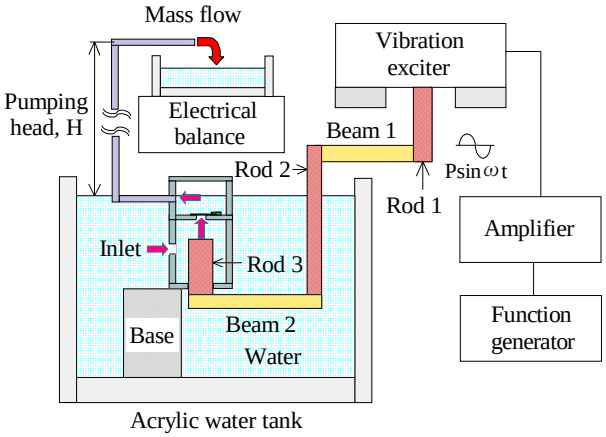

Fig. 9 Details of the experimental setup

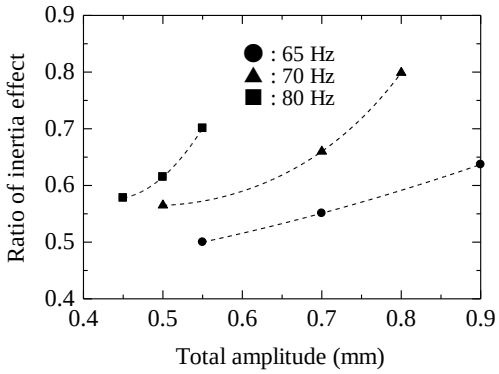

Fig. 10 Relationship between total displacement and ratio of inertia effect

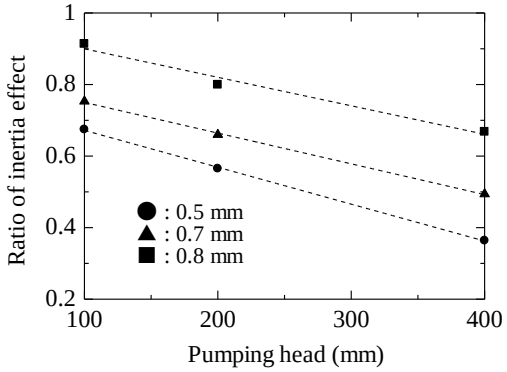

Fig. 11 Relationship between pumping head and ratio of inertia effect

beams, and three rods were connected and inserted into the casing of the pump.

As shown in Fig. 9, when forced displacement is generated by the exciter, rod 3 is displaced. The acrylic rod attached to the vibration component, and rod 3 has the same dimensions. In addition, the casing and valve have the same dimensions as the optimized vibration-type pump. The vibration displacement of rod 3 was substituted by measuring the displacement of beam 1 using a laser displacement meter and a digital oscilloscope.

When the vibration component vibrates at a frequency, f (Hz), the change in the flow rate characteristics due to the displacement amplitude was investigated. For the purpose of clarifying the operation of this pump, the ratio of the inertial effect was defined as follows:

$$I_r = (Q / f) / V, \quad V = 2a\pi d^2 \qquad (1)$$

where I_r is the ratio to the volume, V (mm^3), when the acrylic rod with radius d (mm) vibrates with a total amplitude of 2a (mm) and a flow rate per second of Q (mm^3/s).

Fig. 10 shows the ratio, I_r, of the inertia effect by changing the drive frequency of the exciter when the pumping head, H, is set to 200 mm. As the total amplitude increases, the inertial effect increases. In addition, when the frequency is 70 Hz and the total amplitude is 0.8 mm, approximately 80% of the volume, V, of water due to vibration is discharged.

Fig. 11 shows the pumping head, H, and the ratio, I_r, of the inertial effect by changing the total amplitude of rod 3 when the drive frequency is 70 Hz. The inertial effect decreases as the pumping head, H, increases. On the other hand, when the pumping head is H = 100 mm, the ratio I_r of the inertial effect exceeds 90%, and approximately the same volume of water as the volume due to vibration displacement can be discharged. The obtained results are summarized as follows:

1) The inertial effect is proportional to the increase in drive frequency.

2) As the amplitude of the vibration component increases, the inertial effect increases.

3) When the pump head, H, is low, even if there is a clearance between the rod and the casing, the same amount of water as the volume due to the total amplitude of vibration can be discharged.

6. FLOW CHARACTERISTICS OF THE OPTIMIZED VIBRATION-TYPE PUMP

As shown in Fig. 1, an underwater insertion-type pump with three shape optimizations was prototyped and tested. The drive frequency of the vibration component is 70 Hz. The efficiency, η, of the pump is expressed as follows:

$$\eta = 100 \times M_f \, g \, H / P \, t \qquad (2)$$

where M_f (kg) is the mass flow, g (m/s^2) is the acceleration due to gravity, H (m) is the pumping head, P (W) is the input power to the electromagnet, and t (s) is the measurement time. The mass flow was measured with an electronic balance.

Figs. 12 and 13 show the relationships between the input power to the electromagnet and,

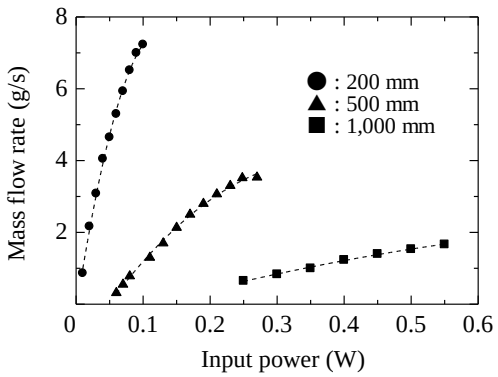

Fig. 12 Relationship between input power and flow rate (underwater-type pump)

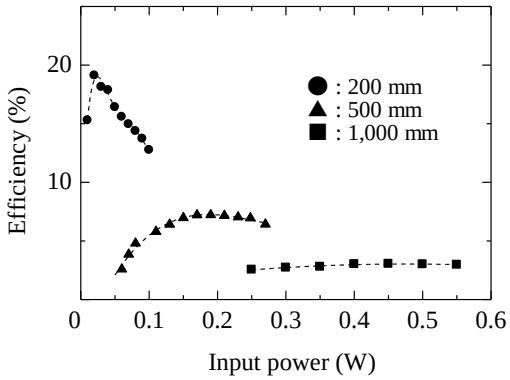

Fig. 13 Relationship between input power and efficiency (underwater-type pump)

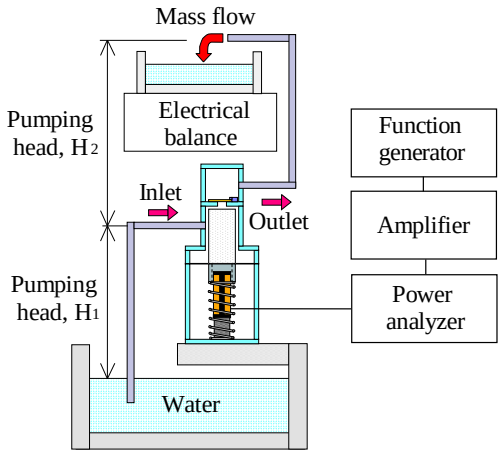

Fig. 14 Outline of the one-valve normal-type pump

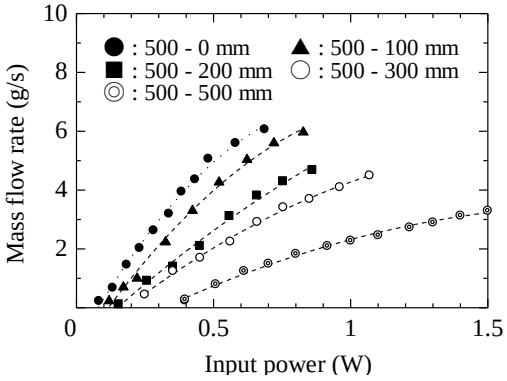

Fig. 15 Relationship between input power and mass flow rate (normal-type pump)

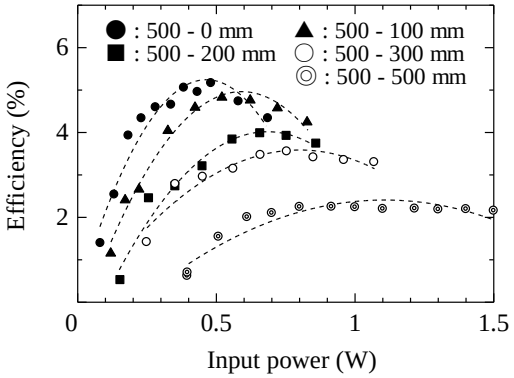

Fig. 16 Relationship between input power and efficiency (normal-type pump)

respectively, the flow rate per second and efficiency by changing the pumping head, H. The flow rate increases approximately linearly as the input power increases. Furthermore, when the pumping head is H = 1,000 mm, approximately 1.8 g of water can be discharged per second. On the other hand, when the input power is 0.02 W and the pumping head is H = 200 mm, the maximum efficiency of this pump is 19.1%. This is because the inertia effect of the acrylic rod is acting. Due to the inertial effect, when the pumping head, H, is low, the efficiency of the prototype pump is significantly higher than that of commercial products.

As a normal application of the pump, an acrylic pipe with an inner diameter of 6 mm was attached to the inlet, as shown in Fig. 14, and the flow rate characteristics of the pump were investigated.

Figs. 15 and 16 show the relationships between the input power to the electromagnet and, respectively, the flow rate per second and efficiency by varying the pumping head (H_1 = 500 mm) and H_2 from 0 mm to 500 mm. The prototype one-valve pump can discharge 2.16 g of water per second at a pumping head of 1,000 mm. The maximum efficiency was approximately 5.1% at an input power of 0.38 W when the total pumping head, H (= $H_1 + H_2$), was 500 mm.

7. CONCLUSIONS

A small one-valve electromagnetic-vibration underwater insertion-type pump was proposed, and the optimum shape of the pump was designed. When this vibration-type pump was inserted into water, the pump had a maximum efficiency of 19.1%. Furthermore, the operating principle of this pump was clarified experimentally, and the effect of the inertial effect of water was clarified.

As a normal application of the prototype pump, an acrylic pipe was attached to the inlet port, and the suction characteristics of the pump were examined. The maximum efficiency of this pump was 5.1%, which was shown to exceed that of commercially available pumps. This vibration-type pump has a very simple structure and can send water exceeding 1,000 mm to the pumping head.

The proposed pump can be used in two ways depending on the application. The underwater insertion-type pump can be applied to circulation in water tanks and cooling devices, and the

normal-type pump can be applied to specific industrial applications. In addition, these vibration-type pumps can be directly driven by the power of a power outlet by tuning the resonance frequency of the vibration component.

8. REFERENCES

[1] Momosaki S., Usami S., Watanabe S. and Okuma K., Experimental Study on Rotational Speed Control of Contra-Rotating Axial Flow Pump, Journal of TSJ, Vol. 39, No. 2, pp.119-125 (2011).

[2] Shigemitsu T., Fukutomi J., Takumi M. and Masahiro S., Unsteady Flow Condition of Centrifugal Pump for Low Viscous Fluid Food, International Journal of Fluid Machinery and Systems, Vol. 10, No. 4, pp. 432-438 (2017).

[3] Yasuyuki N. and Junichiro F., Effect of Impeller Outlet Width on Radial Thrust of Single-Blade Centrifugal Pump with a Helical Spiral Suction Flow Channel, Journal of TSJ, Vol. 39, No. 1, pp. 47-56 (2011).

[4] Benra F., Experimental Investigation of Hydrodynamic Forces for Different Configurations of Single-Blade Centrifugal Pumps, The 11International Symposium on Transport Phenomena and Dynamics of Rotating Machinery (ISROMAC-11), pp. 24-30 (2011).

[5] Kang Y. and Vu H., A newly developed rotor profile for lobe pumps: Generation and numerical performance assessment, Journal of Mechanical Science and Technology, Vol. 28, No. 3, pp. 915-926.(2014).

[6] Kang Y., Vu H. and Hsu H., Factors impacting on performance of lobe pumps, A numerical evaluation, J. Mech., Vol. 28, No. 2, pp. 229-238 (2012).

[7] Houzeaux G., and Codina R., A finite element method for the solution of rotary pumps, Computer. Fluids, Vol. 36, pp. 667-679 (2007).

[8] Voorde J., Vierendeels J. and Dick E., Flow simulations in rotary volumetric pumps and compressors with the fictitious domain method, Computer. Method Appl. Math., Vol. 168, pp. 491-499 (2004).

[9] Kim J., Kan C. and Kim Y., A disposable polydimethylsiloxane – baseddiffuser pump actuated by piezoelectric-disc, Microelectron. Eng.,Vol. 71, No. 2, pp. 119-124 (2004).

[10] Sateesh J., Rao K., Sravani K., Guha K. and Kumar R., Design and Optimization of MEMS Based Piezo-ElectroMicro Pump,4th International Conference on Microelectronics, pp. 1200-1206 (2017).

[11] Yan Q., Yin Y., Sun W. and Fu J., Advances in Valveless Piezoelectric Pumps, Applied science, Vol. 11, No. 15, pp. 1-12 (2021).

[12] Yaguchi H., Mishina T. and Ishikawa K., A New Type of Magnetic Pump with Coupled Mechanical Vibration and Electromagnetic Force, Journal of Mechanical Engineering and Sciences, Vol. 13, No. 3, pp 5212 - 5227 (2019).

[13] Yaguchi H. and Sakuma S., Improvement of a Magnetic Actuator Capable of Movement on a Magnetic Substance, IEEE Transactions on Magnetics, Vol. 52, No. 7, pp.1-4 (2016).

[14] Yaguchi H. and Izumikawa T.**,** Wireless In-Piping Actuator Capable of High-Speed Locomotion by a New Motion Principle, IEEE/ASME Transactions on Mechatronics, Vol. 18, No. 4, pp. 1367 – 1376 (2013).

[15] Yaguchi H., New type of electromagnetically propelled vibration actuator for appearance inspection of iron structure, International Journal of GEOMATE, Vol. 20, No. 77, pp. 69 - 76 (2021).